



Contents lists available at ScienceDirect

Chinese Chemical Letters

journal homepage: [www.elsevier.com/locate/ccllet](http://www.elsevier.com/locate/ccllet)

## A new class of crystalline X-ray induced photochromic materials assembled from anion-directed folding of a flexible cation

Hong-Jin Liao<sup>a,b,c</sup>, Zhu Zhuo<sup>a,b,c,d,\*</sup>, Qing Li<sup>a,c</sup>, Yoshihito Shiota<sup>e</sup>, Jonathan P. Hill<sup>f,\*</sup>, Katsuhiko Ariga<sup>f</sup>, Zi-Xiu Lu<sup>a,c</sup>, Lu-Yao Liu<sup>a,c</sup>, Zi-Ang Nan<sup>a,c</sup>, Wei Wang<sup>a,c</sup>, You-Gui Huang<sup>a,b,c,d,\*</sup>

<sup>a</sup> CAS Key Laboratory of Design and Assembly of Functional Nanostructures, and Fujian Provincial Key Laboratory of Nanomaterials, Fujian Institute of Research on the Structure of Matter, Chinese Academy of Sciences, Fuzhou 350002, China

<sup>b</sup> College of Chemistry and Materials Science, Fujian Normal University, Fuzhou 350007, China

<sup>c</sup> Xiamen Key Laboratory of Rare Earth Photoelectric Functional Materials, Xiamen Institute of Rare Earth Materials, Haixi Institutes, Chinese Academy of Sciences, Xiamen 361021, China

<sup>d</sup> Fujian Science & Technology Innovation Laboratory for Optoelectronic Information of China, Fuzhou 350108, China

<sup>e</sup> Institute for Materials Chemistry and Engineering, Kyushu University, Fukuoka 819-0395, Japan

<sup>f</sup> World Premier International (WPI) Center for Materials Nanoarchitectonics (MANA), National Institute for Materials Science (NIMS), Ibaraki 305-0044, Japan

### ARTICLE INFO

#### Article history:

Received 25 June 2023

Revised 1 August 2023

Accepted 3 September 2023

Available online 5 September 2023

#### Keywords:

Supramolecular

Photochromic

X-ray induced

Anion-directed folding

Electron-deficient viologens

### ABSTRACT

Electron-deficient viologens are widely used as ligands or structure-directing agents (SDAs) to synthesize crystalline X-ray induced photochromic materials. Here, a new rational strategy of anion-directed folding a flexible cation  $(\text{H}_2\text{imb})^{2+}$  ( $(\text{H}_2\text{imb})^{2+} = \text{di-protonated 2,3-bis(imidazolin-2-yl)-2,3-dimethylbutane}$ ) has been developed. Electron-donating  $\text{Cl}^-$  and  $(\text{ZnCl}_4)^{2-}$  are used to direct folding a flexible electron-deficient  $(\text{H}_2\text{imb})^{2+}$  cation. Three complexes  $(\text{H}_2\text{imb})(\text{NO}_3)_2$  (**1**),  $(\text{H}_2\text{imb})\text{Cl}_2 \cdot \text{H}_2\text{O}$  (**2**), and  $(\text{H}_2\text{imb})\text{ZnCl}_4$  (**3**) have been synthesized in which  $(\text{H}_2\text{imb})^{2+}$  crystallize in an *anti-conformation*,  $88.8^\circ\text{-gauche}$ , and  $51.8^\circ\text{-gauche}$ , respectively. In contrary to X-ray silent complex **1**, X-ray induced photochromism has been achieved in both complex **2** and **3**. An intermolecular charge-transfer mechanism has been elucidated and the anion directed folding of  $(\text{H}_2\text{imb})^{2+}$  has been validated to be critical to yield colored long-lived charge-separated states.

© 2024 Published by Elsevier B.V. on behalf of Chinese Chemical Society and Institute of Materia Medica, Chinese Academy of Medical Sciences.

X-ray detection has received considerable attention due to the widespread use of X-ray in medical services and industrial crack detection applications [1–4]. Traditional X-ray detection methods rely on complicated instruments, which greatly limit their accessibility and practicality. Therefore, it is on demand to develop an economical and convenient X-ray detection technique. The emergence of X-ray induced photochromic complexes has opened up an avenue toward this important technique, providing direct visual detection of X-ray [5–9].

In recent years, the progress on photochromic complexes is mainly on metal-organic frameworks (MOFs). These MOFs, utilizing viologens as ligands or structure-directing agents (SDAs), have exhibited promising photochromic behaviors [10–13]. However, the structure change in these MOFs before and after X-ray induced

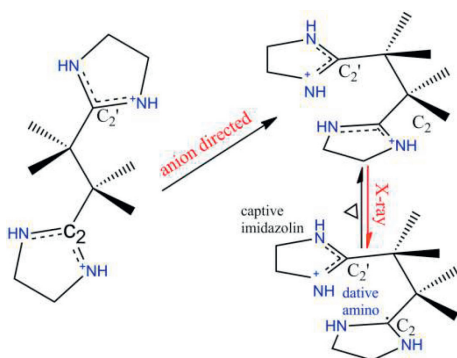
photochromism is usually too subtle to be detected [14,15] because the photochromic reaction can occur only near the surface of the materials except an exceptional framework [13] reported by Zhang *et al.*, and understanding their structure-related chromic behavior by theoretical calculation is also hindered for structural complexities.

In this context, X-ray induced photochromic organic molecules or salts may outperform MOFs because their relatively simple structures may make it feasible to investigate their photochromic processes by theoretical calculation [16]. This provides an opportunity to gain insights into the correlation between structure and photochromism. Therefore, it is highly desirable to develop rational strategies for X-ray induced photochromic organic molecules or salts yet remains a great challenge.

To address this issue, we aimed to develop a supramolecular approach. Herein we demonstrate a rational strategy of precise conformational control of an oxidative cation directed by anions. Photo-induced charge transfer has been demonstrated to be an ef-

\* Corresponding authors.

E-mail addresses: [zhuozhu@fjirms.ac.cn](mailto:zhuozhu@fjirms.ac.cn) (Z. Zhuo), [Jonathan.HILL@nims.go.jp](mailto:Jonathan.HILL@nims.go.jp) (J.P. Hill), [yghuang@fjirms.ac.cn](mailto:yghuang@fjirms.ac.cn) (Y.-G. Huang).



**Scheme 1.** The concept of anion directed folding  $(H_2imb)^{2+}$  leading to the postulated captodative effect for stabilizing the X-ray induced  $(H_2imb)^{\bullet+}$  radical.

fective approach for photochromism, in this regard, the key issue is to design appropriate electron [donor–acceptor] system and stabilize the yielded radicals [10–20].  $(H_2imb)^{2+}$  which can be readily synthesized from  $(H_2azoimp)^{2+}$  through a radical-radical cross-coupling [21,22] attracted our attention, because it is oxidative so that cyclic alkyl amino carbene (CAAC) radical  $(H_2imb)^{\bullet+}$  might be obtained by one electron reduction, as the synthesis of stable N-Heterocyclic carbene (NHC) radicals reported recently [23]. On the other hand, the great flexibility of  $(H_2imb)^{2+}$  allows it to respond to the special geometry demands of counter anions [24,25]. We envisaged that X-ray induced metastable  $(H_2imb)^{\bullet+}$  could be achieved by using various electron-donating anions with different geometries to modulate the conformation of  $(H_2imb)^{2+}$  (Scheme 1).

We were able to synthesize single crystals of  $(H_2imb)(NO_3)_2$  (**1**) (Table S1 in Supporting information) by refluxing the mixture of  $(H_2azoimp)Cl_2$  and  $Co(NO_3)_2 \cdot 6H_2O$  in methanol followed by crystallization through slow solvent evaporation ( $(H_2azoimp)Cl_2 = (2,2'$ -azobis[2-(2-imidazolin-2-yl)propane]dihydrochloride). In complex **1**,  $(H_2imb)^{2+}$  crystallize in an *anti*-conformation with the  $C_2$ – $C_2'$  distance (the distance between the central C atoms of imidazolium moieties) of 3.833 Å and are connected into a one-dimensional ribbon by  $NO_3^-$  through [N–H...O] hydrogen bonds (Fig. 1a). The PXRD pattern and IR spectrum for complex **1** are shown in Figs. S1 and S2 (Supporting information), respectively. Complex **1** is X-ray silent (Fig. S3 in Supporting information) probably because of the poor electron donating performance of  $NO_3^-$  and/or poor stability of postulated *anti*- $(H_2imb)^{\bullet+}$ . This finding promoted us to modulate the conformation of  $(H_2imb)^{2+}$  with  $Cl^-$  or  $Cl^-$  containing anions for their greater electron donating performance. The following couple of advantages could be benefited from this strategy: (1)  $Cl^-$  has been demonstrated as an excellent X-ray induced electron donor while that of  $NO_3^-$  has rarely been found [10,26], thus  $[Cl^--(H_2imb)^{2+}]$  would be a better electron [donor–acceptor] system than  $[NO_3^--(H_2imb)^{2+}]$ ; (2)  $(H_2imb)^{2+}$  might be folded to *syn*- $(H_2imb)^{2+}$  by  $Cl^-$  or  $Cl^-$  containing anions. Since both the captive imidazolium moiety and the dative alkyl amino groups are close to the central C atom in *syn*- $(H_2imb)^{\bullet+}$  (Scheme 1), the captodative effect resulted from the synergy of the electron drawing of the imidazolium moiety and the electron pulling of the alkyl amino groups is beneficial for stabilizing *syn*- $(H_2imb)^{\bullet+}$  [27–29]. As if absorption bands of the X-ray induced charge separated species appear in visible region, X-ray induced photochromism could be achieved. To validate our postulation, we used  $Cl^-$  and  $(ZnCl_4)^{2-}$  to direct folding of  $(H_2imb)^{2+}$ .

Crystals of  $(H_2imb)Cl_2 \cdot H_2O$  (**2**) were synthesized by refluxing  $(H_2azoimp)Cl_2$  in methanol followed by recrystallizing in  $H_2O$ . In complex **2**,  $(H_2imb)^{2+}$  is folded into a *gauche* conformation (Fig. 1b) with the dihedral angle between imidazolium moieties

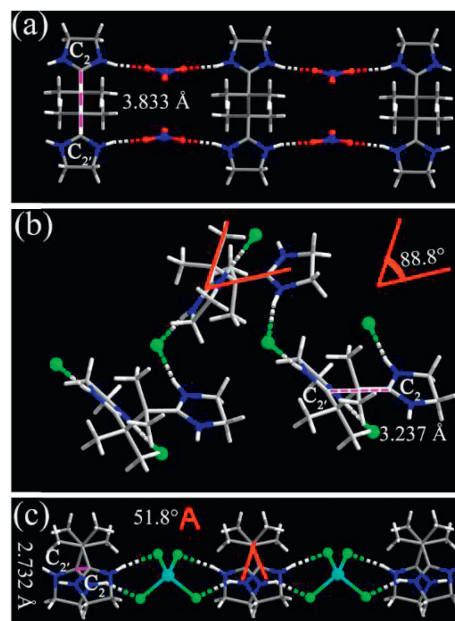


**Fig. 1.** (a) The ribbon structure of complex **1**. (b) The hydrogen bonded chain in complex **2**. (c) The chain structure of complex **3** (Zn cyan, Cl green, O red, N blue, C gray, H white).

**Table 1**

Comparison of  $C_2$ – $C_2'$  distance and the dihedral angle between imidazolium moieties of compounds **1**, **2**, and **3**.

Complex	$C_2$ – $C_2'$ distance (Å)	Dihedral angle (°)
<b>1</b>	3.833	180
<b>2</b>	3.237	88.8
<b>3</b>	2.732	51.8

of 88.8° and the  $C_2$ – $C_2'$  distance of 3.237 Å.  $(H_2imb)^{2+}$  are assembled into one dimensional chains by  $Cl^-$  through N–H...Cl hydrogen bonds which are further assembled into a three dimensional framework structure by  $H_2O$  molecules through N–H...O and O–H...Cl hydrogen bonds (Fig. S4 in Supporting information).

To enhance the postulated captodative effect in  $(H_2imb)^{\bullet+}$ , we then aimed to further shorten the  $C_2$ – $C_2'$  distance by further folding the cation with  $Cl^-$  containing anions. We envisaged that anions with tetrahedral geometries would direct  $(H_2imb)^{2+}$  to crystallize in an approximately *syn* conformation for intermolecular hydrogen bonds, therefore  $(H_2imb)ZnCl_4$  (**3**) was synthesized by refluxing the mixture of  $(H_2azoimp)Cl_2$  and  $ZnCl_2$  in methanol (Fig. S5 in Supporting information). Compared with those in complex **2**,  $(H_2imb)^{2+}$  in complex **3** are further folded into a *gauche* conformation with the dihedral angle between imidazolium moieties of 51.8° (Fig. 1c) and the  $C_2$ – $C_2'$  distance of 2.732 Å.  $(H_2imb)^{2+}$  are assembled into a one-dimensional supramolecular chain by  $(ZnCl_4)^{2-}$  anions through N–H...Cl hydrogen bonds. Remarkably, complex **1** can transit to complex **3** and complex **2** can transit to complexes **1** and **3** by anion exchange. The  $C_2$ – $C_2'$  distance has been shortened from 3.833 Å in complex **1** to 2.732 Å in complex **3**, thus great  $(H_2imb)^{\bullet+}$  stability enhancement can be expected [27].

With the directing effect of different anions, the conformation of  $(H_2imb)^{2+}$  has been successfully modulated. The main structural parameters related to the conformation of  $(H_2imb)^{2+}$  are listed in Table 1. To examine whether our design strategy is effective for photochromic complexes, crystalline powder samples of complex **2** and **3** were irradiated with soft X-ray (Cu-K $\alpha$ ,  $\lambda = 1.54056$  Å, 0.6 kW) on a powder X-ray diffractometer. Both complexes showed

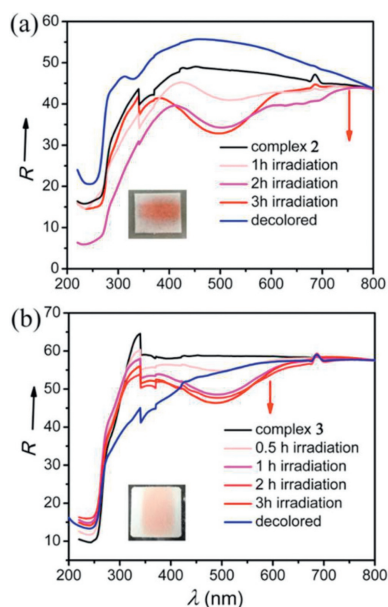


**Fig. 2.** Time-dependent UV-vis diffuse reflectance spectra of complex (a) **2** and (b) **3**, showing the color change of complex (a inset) **2** and (b inset) **3** upon X-ray irradiation for 3 h and 10 h, respectively.

a noticeable color change from colorless to red in 0.5 h upon irradiation at room temperature and the color became deeper and deeper with increasing exposure time (Figs. S6 and S7 in Supporting information). The sensitivities (Obvious color change can be observed within 0.5 h with an X-ray source of 0.6 kW) of complex **2** and **3** to X-ray are comparable to other X-ray induced photochromic materials (Table S2 in Supporting information) [11–13]. The color of both the red photoproducts could slowly fade in approximate one month in atmosphere condition, and full decoloration could be completed in 2 h by annealing at 130 °C. Decoloration of complex **2** at 130 °C for 2 h gives rise to pale yellow dehydrated **2** ( $\text{H}_2\text{imb}\text{Cl}_2$ ) as indicated by Thermogravimetric (TG) analysis (Fig. S8 in Supporting information). Although the crystals of dehydrated **2** were not suitable for single-crystal X-ray structural determination, PXRD measurement indicated that the one-dimensional hydrogen bonded chains assembled from  $\text{Cl}^-$  bridged ( $\text{H}_2\text{imb}\text{Cl}_2$ ) remain after dehydration (Fig. S9 in Supporting information), indicating the photochromism is not related to the lattice  $\text{H}_2\text{O}$  molecule (Figs. S10 and S11 in Supporting information). In comparison with the colorless samples of complexes **2** and **3**, a new broad band centered at  $\sim 487$  nm emerges in the time-dependent UV-vis spectra of both the red photoproducts which increases with prolonged irradiation time and disappears after decoloration (Fig. 2). This absorption band is characteristic of CAAC radicals [23,30,31]. Dehydrated **2** shows similar photochromic behavior. The reversible coloration-decoloration processes for both complexes can be repeated for at least three cycles (Figs. S12 and S13 in Supporting information) while the structures remain almost unchanged as revealed by SCXRD, PXRD (Figs. S5 and S14 in Supporting information) and IR analyses (Figs. S15 and S16 in Supporting information). Coloration of both complexes also can be induced by soft X-ray ( $\text{Al-K}\alpha$ ,  $\lambda = 8.357$  Å) (Fig. S17 in Supporting information), but no obvious color change can be observed upon UV irradiation.

X-ray photoelectron spectroscopy (XPS) measurements were performed on complexes **2** and **3** before and after coloration to get insights into the mechanism of the photochromic behavior. Early studies indicated that the photochromism of viologen halides is usually induced by charge-transfer from halide to viologen [10,13,26], therefore X-ray induced charge-transfer from  $\text{Cl}^-$

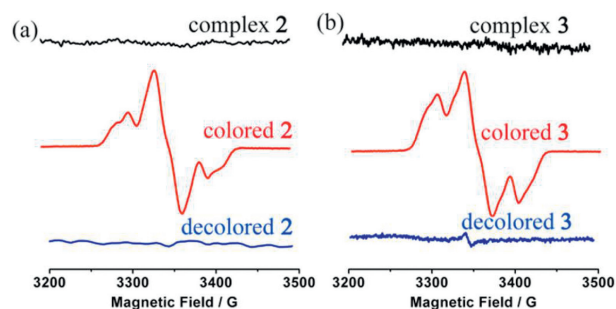


**Fig. 3.** ESR spectrum evolution of complex (a) **2** and (b) **3** upon coloration-decoloration processes.

to ( $\text{H}_2\text{imb}\text{Cl}_2$ ) $^{2+}$  and core-level spectra variation of Cl 2p, C 1s, and N 1s can be expected before and after X-ray irradiation. Indeed, the core-level spectra of Zn 2p of complex **3** were almost the same before and after coloration, while the variation in the core-level spectra of Cl 2p, C 1s, and N 1s of both complexes is discernible (Figs. S18–S21 in Supporting information). For both complexes, the spectra of Cl 2p and N 1s slightly shift toward high binding energy region after coloration, while the spectra of C 1s slightly shift toward low binding energy region (Tables S3 and S4 in Supporting information).  $\text{Cl}^-$  is electron-rich and ( $\text{H}_2\text{imb}\text{Cl}_2$ ) $^{2+}$  is electron-deficient, therefore the charge transferred from  $\text{Cl}^-$  to ( $\text{H}_2\text{imb}\text{Cl}_2$ ) $^{2+}$  generating open-shelled  $\text{Cl}^\cdot$  and ( $\text{H}_2\text{imb}\text{Cl}_2$ ) $^{\cdot+}$  radicals upon X-ray irradiation.

To characterize the feature of the yielded radical species, X-band electron spin resonance (ESR) spectroscopy and magnetic measurements were also performed on colorless and colored complexes **2** and **3**. As shown in Fig. 3, colorless complex **2**, complex **3** are ESR silent, but a typical broaden triplet-state signal [32–34] emerged with a zero-field parameter of  $D = 6.2$  mT and  $E = 1.5$  mT for colored complex **2** and  $D = 7.2$  mT and  $E = 1.9$  mT for colored complex **3**, as determined by spectrum simulation (Fig. S22 in Supporting information). Both the  $g$  factors are anisotropic with  $g_x = 2.0026$ ,  $g_y = 2.0082$ ,  $g_z = 2.0045$  for colored **2** and  $g_x = 2.0022$ ,  $g_y = 2.0062$ ,  $g_z = 2.0052$  for colored **3**, respectively. The average spin–spin distance was estimated from  $D$  to be 7.61 Å for colored **2** and 7.26 Å for colored **3**, respectively. The magnetic susceptibilities of colored complexes **2** and **3** obtained through X-ray irradiation of original samples for 3 h were measured under an applied field  $H = 1$  kOe, after the color completely faded the magnetic susceptibilities were measured again under the same condition. In such way, the data allow subtraction of the diamagnetic contribution from the sample holders and the intrinsic diamagnetism of the samples. The  $\chi_{mT}$  values for both colored **2** and **3** decrease linearly upon cooling indicating dominant antiferromagnetic interaction between spins (Fig. S23 in Supporting information) [35,36]. The field dependence of magnetization for colored **2** and **3** at 2.0 K saturated at high fields suggesting unidirectionally aligned spins were developed across the materials (Figs. S24 and S25 in Supporting information) [37].

To clarify whether the folding of ( $\text{H}_2\text{imb}\text{Cl}_2$ ) $^{2+}$  in complex **2** and **3** is crucial for the X-ray induced photochromism, density functional theory (DFT) calculations were performed at the B3LYP/6-311+G\*\* level using the Gaussian 09 program package [38] to shed light on the electronic structures of colored **2** and **3** (Fig. S26 in Supporting information). For both complexes, DFT calculations suggest the highest occupied molecular orbital (HOMO) and the lowest unoccupied molecular orbital (LUMO) are located on  $\text{Cl}^-$  and the two  $\pi$ -systems of ( $\text{H}_2\text{imb}\text{Cl}_2$ ) $^{2+}$ , respectively (Fig. S27 in Supporting information). The energy differences  $\Delta E_{\text{BT-CS}}$  between the biradical triplet state (BT) and closed-shell state (CS) were calculated to be 3.3 eV and 2.4 eV for complex **2** and **3**, respectively. The

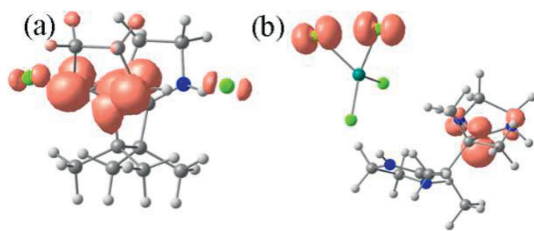


Fig. 4. Spin densities of (a) colored **2** and (b) **3** calculated at B3LYP/6-311+G\*\* level.

$\Delta E_{\text{BT-CS}}$  value for complex **1** was also calculated, giving a value of 4.36 eV which is higher than those of complex **2** and **3**. This result implies the triplet state of complex **1** is not stable and probably too short-lived to be detected by naked eyes. The spin densities of triplet complex **2** and **3** are distributed on both the Cl and  $(\text{H}_2\text{imb})^{+\bullet}$  radicals, and the spin densities on  $(\text{H}_2\text{imb})^{+\bullet}$  are delocalized (Fig. 4). To give further insights into the photochromic behaviours, the electron transition configurations of complex **2** were calculated (Table S5 in Supporting information). Several significant HOMO→LUMO transition configurations (amplitude  $f$  larger than 0.04) can be identified, suggesting the observed X-ray induced photochromism originating from HOMO→LUMO charge transfer.

In summary, X-ray induced photochromism has been achieved on two organic salts designed by anion-directed folding a flexible cation. The photo responsive mechanism has been elucidated on the basis of UV-vis, ESR, XPS measurements, and DFT calculations. This work has developed a new class of X-ray induced photochromic materials, demonstrated that anion directed precise conformational control of cations is critical for the functionalities, therefore opened a new avenue for design of X-ray induced photochromic materials.

#### Declaration of competing interest

The authors declare that they have no known competing financial interests or personal relationships that could have appeared to influence the work reported in this paper.

#### Acknowledgments

This research was supported by National Natural Science Foundation of China (No. 92261109), Natural Science Foundation of Fujian Province (No. 2020J05080), Project Funded by China Postdoctoral Science Foundation (No. 2023M733496), Natural Science Foundation of Xiamen (No. 3502Z20206080), Fujian Science & Technology Innovation Laboratory for Optoelectronic Information of China (No. 2021ZR110), Recruitment Program of Global Youth Experts, Youth Innovation Promotion Association CAS (No.

2021302). A portion of this work was performed on the Steady High Magnetic Field Facilities, High Magnetic Field Laboratory, CAS.

#### Supplementary materials

Supplementary material associated with this article can be found, in the online version, at doi:10.1016/j.ccl.2023.109052.

#### References

- [1] V. Kiryukhin, D. Casa, J.P. Hill, et al., *Nature* 386 (1997) 813–815.
- [2] V. Kiryukhin, Y. Horibe, Y.S. Hor, et al., *Phys. Rev. Lett.* 97 (2006) 225503.
- [3] G. Poneti, M. Mannini, L. Sorace, et al., *Angew. Chem. Int. Ed.* 49 (2010) 1954–1957.
- [4] K.D. Irwin, G.C. Hilton, D.A. Wollman, et al., *Appl. Phys. Lett.* 69 (1996) 1945–1947.
- [5] J.A. Sobrinho, J.H.K.S. Monteiro, M.R. Davolos, et al., *ChemistrySelect* 2 (2017) 3538–3548.
- [6] K. Kinashi, Y. Miyamae, R. Nakamura, et al., *Chem. Commun.* 51 (2015) 11170–11173.
- [7] B.D. Ge, Y. Han, S.D. Han, et al., *Inorg. Chem. Front.* 6 (2019) 2435–2440.
- [8] P.F. Hao, X. Liu, C.Y. Guo, et al., *Inorg. Chem. Front.* 9 (2022) 879–888.
- [9] D. Gupta, A.K. Gaur, D. Chauhan, et al., *Inorg. Chem. Front.* 9 (2022) 2315–2327.
- [10] M.S. Wang, C. Yang, G.E. Wang, et al., *Angew. Chem. Int. Ed.* 51 (2012) 3432–3435.
- [11] J.B. Wu, C.Y. Tao, Y. Li, et al., *Chem. Sci.* 5 (2014) 4237–4241.
- [12] H. Zhang, X.T. Wu, *Adv. Sci.* 3 (2016) 1500224.
- [13] C. Chen, J.K. Sun, Y.J. Zhang, et al., *Angew. Chem. Int. Ed.* 56 (2017) 14458–14462.
- [14] J.Z. Qiu, Y. Yu, Z.F. Chen, et al., *Chin. Chem. Lett.* 34 (2023) 107346.
- [15] Q. Zhang, J.X. Hu, Q. Li, et al., *Chin. Chem. Lett.* 33 (2022) 1417–1421.
- [16] T. Yamaguchi, Y. Kobayashi, J. Abe, *J. Am. Chem. Soc.* 138 (2016) 906–913.
- [17] J.Z. Liao, S.S. Wang, X.Y. Wu, et al., *Dalton Trans.* 47 (2018) 1027–1031.
- [18] M. Morimoto, S. Kobatake, M. Irie, *Chem. Commun.* (2006) 2656–2658.
- [19] P.X. Li, M.S. Wang, M.J. Zhang, et al., *Angew. Chem. Int. Ed.* 53 (2014) 11529–11531.
- [20] C. Sun, G. Xu, X.M. Jiang, et al., *J. Am. Chem. Soc.* 140 (2018) 2805–2811.
- [21] Y.I. González, M. Stjern Dahl, D. Danino, *Langmuir* 20 (2004) 7053–7063.
- [22] D. Spaccini, N. Pastori, A. Clerici, et al., *J. Am. Chem. Soc.* 130 (2008) 18018–18024.
- [23] D. Rottschäfer, B. Neumann, H. Stammer, et al., *Angew. Chem. Int. Ed.* 57 (2018) 4765–4768.
- [24] H. Maeda, Y. Bando, *Chem. Commun.* 49 (2013) 4100–4113.
- [25] Y. Haketa, Y. Bando, K. Takaishi, et al., *Angew. Chem. Int. Ed.* 51 (2012) 7967–7971.
- [26] G. Xu, G.C. Guo, M.S. Wang, et al., *Angew. Chem. Int. Ed.* 46 (2007) 3249–3251.
- [27] E.V. Anslyn, D.A. Dougherty, *Modern Physical Organic Chemistry*, Sausalito, CA, 2005.
- [28] H.G. Viehe, Z. Janousek, R. Merenyi, et al., *Acc. Chem. Res.* 18 (1985) 148–154.
- [29] J.R. David, R. Brook, C. Haltiwanger, *J. Am. Chem. Soc.* 113 (1991) 5910–5913.
- [30] M.M. Hansmann, M. Melaimi, G. Bertrand, *J. Am. Chem. Soc.* 140 (2018) 2206–2213.
- [31] M.M. Hansmann, M. Melaimi, D. Munz, et al., *J. Am. Chem. Soc.* 140 (2018) 2546–2554.
- [32] T. Nozawa, M. Nagata, M. Ichinohe, et al., *J. Am. Chem. Soc.* 133 (2011) 5773–5775.
- [33] Y.T. Su, X.Y. Wang, Y.T. Li, et al., *Angew. Chem. Int. Ed.* 54 (2015) 1634–1637.
- [34] T. Li, G.W. Tan, D. Shao, et al., *J. Am. Chem. Soc.* 138 (2016) 10092–10095.
- [35] C.P. Constantinides, A.A. Berezin, M. Manoli, et al., *Chem. Eur. J.* 20 (2014) 5388–5396.
- [36] X.Y. Li, Y. Zou, S.D. Han, et al., *Inorg. Chem. Front.* 8 (2021) 4186–4191.
- [37] E.Q. Jin, M. Asada, Q. Xu, et al., *Science* 357 (2017) 673–676.
- [38] M.J. Frisch, G.W. Trucks, H.B. Schlegel, et al., *Gaussian 09, Revision E. 01*, Gaussian, Inc., Wallingford CT, 2004.